

## **Development of ELF Receiver System for Observation of Electromagnetic Phenomena Associated with Earthquakes or Volcanic Eruptions**

Ichiro TOMIZAWA and Takeo YOSHINO

### **Abstract**

Development of ELF receiver system for observation of electromagnetic(EM) phenomena associated with crustal deformations such as earthquake or volcanic eruption is described in this paper. The receiver system is designed based on the experimental data which has been obtained in the network observation developed around the Kanto district. The design is mainly focused on dynamic range, reduction of interference from the commercial power system, stability and operability of the receiver system. The frequency characteristics and the input-to-output characteristics are obtained from the performance test of the assembled receiver sub-units. The interference rejection ratio at 60Hz is more than 150dB for both 1525Hz and 36Hz receivers. Those at 1500Hz and 1560Hz, which are the closest harmonic frequencies for 1525Hz, are more than 50dB for the 1525Hz receiver. The stability of the assembled receiver is  $10^{-5}$ /day which can be estimated by that of the oscillator. The newly developed receiver system has been used for the EM observation of the Unzen volcano.

### **1. Introduction**

We have been observing the enhancements of the electromagnetic(EM) noise associated with earthquakes(1-3) or with volcanic eruptions(4-5). These observations have been made mainly at 82kHz. However the most suitable frequency for this observation is not known since the generation mechanism of the EM noise and the propagation characteristics through the ground have not been clearly explained. The first frequency, 82kHz, is selected by chance, because the lower frequency limit of our receiving equipments was 50kHz, and because the frequency was relatively quiet around the Kanto district in 1981 when the cooperative study with the Academy of Science of USSR started(1). However, our main observation frequency goes down to the ELF band since 1991. There are two reasons to move our main observation frequency to lower.

The condition of observation at 82kHz is getting worse year by year due to the increase in the number of equipments utilizing power switching devices or digital circuits(6). Additionally the field strength at 82kHz shows daily variation more than 20 dB in the summer time, which may mask weak increase in the nighttime. This is the first reason why we have to use the other frequencies.

The second reason is that we have been searching for better frequencies for observation based on the three conditions: the background noise level, the possible generation mechanism of EM noise associated with earthquakes, and the estimated propagation loss through the ground. As wide band EM noise can be expected for these possible generation mechanisms(7), and as the propagation loss should be much less for lower frequencies compared to 82kHz when we assumed the plane wave, it is better to use the lower frequencies. Although much lower frequency is better for this reason, the background noise on the ground surface is contaminated by the natural or the artificial EM noises. Below 1Hz the natural EM noise is coming from the source in the ionosphere or in the magnetosphere, and it indicates steep increase in amplitude by decreasing frequency. Above 1Hz the natural EM noise in Japan is mainly atmospheric noise. The intensity of the atmospheric noise is characterized by the propagation in the ground-ionosphere waveguide. A typical background noise between 1Hz and 2kHz, observed at Sugadaira Space Radiowave Observatory of the University of Electro-Communications, is shown in Figure 1. Between 7 and approximately 35Hz, the intensity enhancement can be observed due to the resonance of the cavity resonator produced by the global earth-ionosphere waveguide, which is called the Schumann resonance(8). The Schumann resonance can be seen in Figure 1(b) between 5 and 35Hz as the periodic enhancement of field amplitude. The intensity at these resonance frequencies may vary in time, depending on the ionospheric conditions or on the thunderstorm activities. Above 35Hz up to 1.7kHz, the intensity gradually decreases without any enhancement as shown in Figure 1(a). Above 1.7kHz, as the atmospheric noise can propagate without much loss in magnitude, the background noise increases and shows a peak between 5 and 10kHz. The propagation characteristics vary depending on the local time or on the season. Above 10kHz the intensity decreases in increasing the frequency, however, it varies significantly in local time because of the high

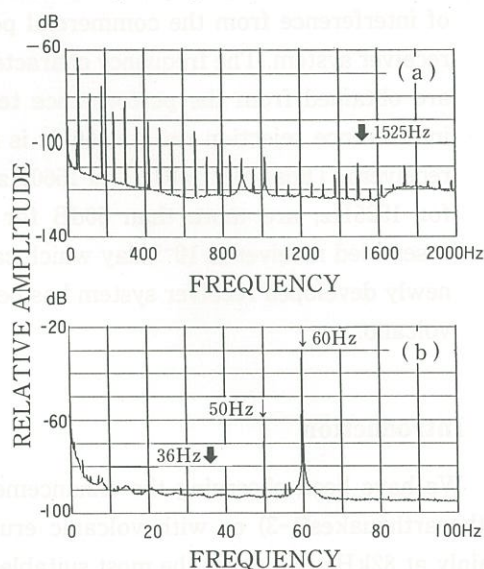


**Fig. 1** Typical frequency spectra of background magnetic field noise observed at Sugadaira Space Radiowave Observatory in Nagano Prefecture. The frequency range of the spectrum is from 0 to 2000Hz for (a), and from 0 to 100Hz for (b). The floor of the noise is mainly contributed by atmospherics propagating over 1000 km, however, the line spectra appeared on the background noise are induction field of the local power lines.

attenuation loss the in daytime. As it is required to detect the weak and abnormal increase in field strength that must exceed the normal fluctuation level of the background noise, it is better to use the most quiet frequency in the background noise, and to use the frequency of the stable amplitude. The most quiet frequency between 1Hz and 10kHz is around 1.5kHz as shown in Figure 1(a). On the other hand, as the most stable in amplitude must be determined by the dependence of the geomagnetic activity, of the local time effect of ionosphere, or of the global thunderstorm activities, the frequency range between 35Hz and 1.7kHz is better compared with other frequency bands. Although we can use wideband receiver for this frequency range under the natural condition, unfortunately we cannot find out such a good location in Japan without contamination with the artificial noise, especially by the power line harmonic fields. So we concluded that the ELF range of frequency, especially between 35Hz and 1.7kHz, is better for this observation if we can escape from the artificial noise by using special techniques for receivers. Therefore we have decided to observe at the bottom and at the top of this ELF range, i. e., 36Hz and 1525Hz, where the harmonic interference of the power lines can be removed by the techniques to be described in the next section. As the level of contamination varies place by place, we must experimentally fix the place of low contamination. Usually it can be said that the better place may be in the range far from the city area and far from power lines.

## 2. Design of receiver system

### 2.1 Basic design of the ELF receiver system

We must observe all EM field components to determine all the characteristics of the wave field. However, we can reduce the number of components if we can fix the characteristics of the wave field to be observed.

We have been observing the field strength of the orthogonal horizontal magnetic fields at 82kHz, since the propagation mode at this frequency might be the surface mode during the daytime and the skywave mode during the nighttime. We have considered that the direct propagation through the ground from the generation source in the ground to the receiver might be small compared to the surface mode or the skywave mode from the actual emission point on the ground surface(3). Therefore we can restrict the propagation to those two modes, then the number of components might be sufficient to describe the propagation.

On the other hand, as the direct propagation through the ground can be possible at ELF, we must observe all field components. However, we can reduce the number of field components to five by assuming that the characteristic of the propagation could be described by the five components.

First, let us describe the characteristics of the ground-ionosphere propagation mode. As the propagation mode is  $TM_0$  which has the vertical electric field and the horizontal magnetic field for the perfect ground, we can reduce the components to three; vertical electric and two orthogonal horizontal magnetic fields. Observation of the vertical electric field is very complicated at ELF since the effective height of the vertical electric field sensor is quite short and the sensor is too sensitive to the surrounding objects. It is better not to use this component for



observation. We can expect the induced horizontal electric fields for the actual ground which has a lower conductivity. If we can compare these horizontal electric fields with the orthogonal magnetic fields, we can manage to describe this propagation mode.

Second, let us describe the characteristics of the direct propagation mode. Although the mode is not explained in detail, we can describe the propagation mode by observing the boundary condition at the ground surface. We can also describe this mode without the vertical electric component.

Third, let us describe the characteristics of the interference. Even though the interference field might have all kind of field components, the location and the characteristic of the interference are usually common to most of the events. If we can fix the characteristics of the interference source without the vertical electric field, we can reduce the number of components. As the interference field usually shows the characteristics of the induction field, which have a predominant field component and a main field direction, it can be easy to discriminate the interference of this kind from the propagation field. However it is impossible to discriminate the interference relatively far from the observation point since the characteristics of the field may be similar to those of the natural noises.

## 2.2 *Receiving frequencies of each field component*

We have been fixed the observation frequencies in the ELF band according to the three criteria as described above. The fixed frequencies are 36Hz and 1525Hz, which are corresponding to the bottom and the top, respectively, of the suitable frequency band, 35Hz to 1.7kHz. The most effective parameter for this frequency selection is the possible selectivity of the receiver at these frequencies.

The interference field strength at 1525Hz, which is always falling between the two harmonic frequencies, 1500Hz and 1550Hz for the 50Hz district, or 1500Hz and 1560Hz for the 60Hz district, must be much higher than that of the background. For example, the relative field strengths at Sugadaira, where the fundamental frequency of the commercial power system is 60Hz, as shown in Figure 1(a) are 15dB for 1500Hz and 5dB for 1560Hz. Therefore we must reduce the amplitude at these harmonic frequencies more than 40dB to observe the background strength without interference.

The interference field strength at 50Hz or 60Hz, which are the fundamental frequency of the Japanese commercial power systems, must be much higher than that of the background. For example, the relative field strength at Sugadaira as shown in Figure 1 is 30dB for 50Hz, and 60dB for 60Hz. The both fundamental frequencies can be seen in this figure since the closest distance to the 50Hz district is approximately 20km from Sugadaira. Therefore we must reduce the amplitude more than 50dB for 50Hz and 80dB for 60Hz for this case. The main attenuation frequency should be determined by the frequency of the power system at the observation point.

As we have planned to use this receiver system at the Unzen Volcano in Nagasaki Prefecture, where the fundamental frequency is 60Hz, we are going to design the receiver system for 60Hz. If we assumed that the interference environment around Unzen Volcano might be similar to that of Sugadaira, the main design parameters for the receiver given above can be

applied for our practical design.

### 2.3 Basic design of the ELF receiver system

The basic block diagram of the ELF receiver system is shown in Figure 2. The receiver system consists of five receiver units. Each of the receiver units includes 1525Hz and 36Hz receiver sub-units. The inputs of the five receiver units are shown on the left side of each receiver unit in Figure 1. The upper three receiver units are connected to the magnetic field sensors and the lower two receiver units to the horizontal electric field sensors. The characteristics of the sensors are not described in detail in this paper, but the summarized characteristics of them are presented in Table 1. Output of the receiver system is in three ways, the DC voltage for a digital recorder, the DC voltage for a pen recorder, and the video signal for a video recorder or for an oscilloscope. This receiver system is also designed in employing sub-units to be easily replaced in field. The basic receiver can be separated into seven sub-units; a power supply, a clock generator, and five receiver units. The assembled feature of this receiver is shown in Figure 3 and its basic specification is indicated in Table 3.

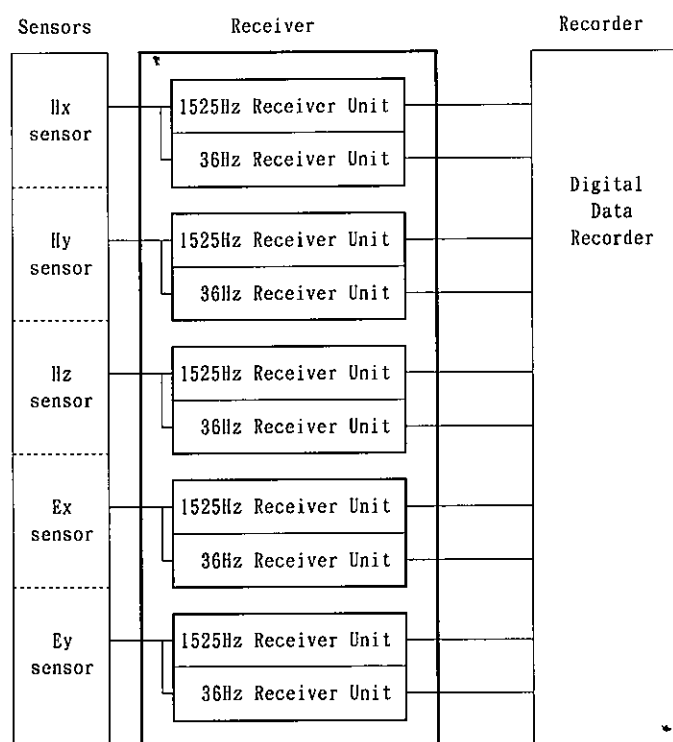


**Fig. 2** A simplified diagram of the combination of the magnetic and the electric field sensors, the ELF receiver units, and the digital data recorder. The ELF receiver consists of five boxes which contain one 1525Hz and one 36Hz receiver units. As all of these five boxes are equivalent in the electrical and the mechanical characteristics, it is quite easy to change each other for inspection of failure or to replace with a spare unit.

**Table 1** Specification of the sensor and the preamplifier. The sensitivities of the sensor and the preamplifier are used to calculate the actual electric or magnetic field strengths from the output voltages of the receiver units.

Sensitive Field Component	Magnetic	Electric
Sensor	Loop Antenna	Electrode Pair
Dimension	30cm x 1cm x 1cm	5m between electrodes
Sensitivity of Sensor		
at 36Hz	19dB(*1)	14dB(*2)
at 1525Hz	19dB(*1)	14dB(*2)
Preamplifier Voltage Gain	20dB	20dB
Background Noise		
at 36Hz	-130dB(*3)	-120dB(*4)
at 1525Hz	-150dB(*3)	-140dB(*4)

Notes:

\*1 indicates that 0dB is  $1V/(A/m/Hz^{1/2})$ .

\*2 indicates that 0dB is  $1V/(V/m/Hz^{1/2})$ .

\*3 indicates that 0dB is  $1A/m/Hz^{1/2}$ .

\*4 indicates that 0dB is  $1V/m/Hz^{1/2}$ .

**Table 2** Basic specification of each receiver unit determined by the experimental data.

Center Frequency	36Hz	1525Hz
3dB Bandwidth	4Hz	5Hz
Equivalent input noise	-90dBV	-120dBV
Dynamic Range	60dB	50dB
Frequency Stability	$10^{-5}/DAY$	$10^{-5}/DAY$
Maximum Frequency Offset	0.1Hz	5Hz
Maximum Interference Reduction		
at 60Hz	>150dB	>150dB
at 180Hz	>120dB	>150dB
at 1500Hz,1560Hz	>150dB	>50dB
Integration Time Constant	10sec	10sec
Input Impedance	100k $\Omega$	100k $\Omega$

**Table 3** Basic specification of the ELF receiver system.

Number of Receiving Units	5ch
Output Voltage	
to Digital Recorder	$\pm 1VDC$
to Pen Recorder	$\pm 3VDC$
to Oscilloscope	$\pm 10Vpp$
DC Power Supply for Preamplifier	$\pm 12VDC$
AC Input	100VAC 0.2A
Weight	25kg
Dimension	52cm x 40cm x 25cm
Operating Temperature	0 to 40°C

## 2.4 Basic design of a receiver unit

Each receiver unit must satisfy the basic specification described in Table 2 according to the requirement on the background EM noise, on the interference, and on the stability. Amplitude gain of the receiver sub-unit is easily determined by calculating difference between the least gain to match the detector voltage range and the equivalent background noise voltage at the input of the receiver sub-unit. The calculations for both frequencies result in 70dB for 1525Hz and 60dB for 36Hz. If we directly amplify the output of the sensors by these gains, the signal must be easily saturated by the limit of the amplifier. Therefore we must reduce the undesired spectral components without distortion for the desired frequency component. The most intense





intense component at the fundamental frequency by 60dB.

The narrow BPF employed in the both sub-units consists of four second-order switched capacitor filters (SCFs). The SCFs are designed to produce a very narrow BPF. For 1525Hz receiver sub-unit, the -3dB and the -40dB bandwidths of the filter are 5Hz and 40Hz, respectively. As the frequency characteristics of SCFs are controlled by the clock frequency which is generated from the common crystal oscillator, the stability of the characteristics is approximately  $10^{-5}$ /day. However, the dynamic range of the SCF is reduced by the internal switching noise. It is required to select the components based on the internal noise characteristic. We have selected LMF100 (manufactured by the National Semiconductor, Co.) instead of MF10 which

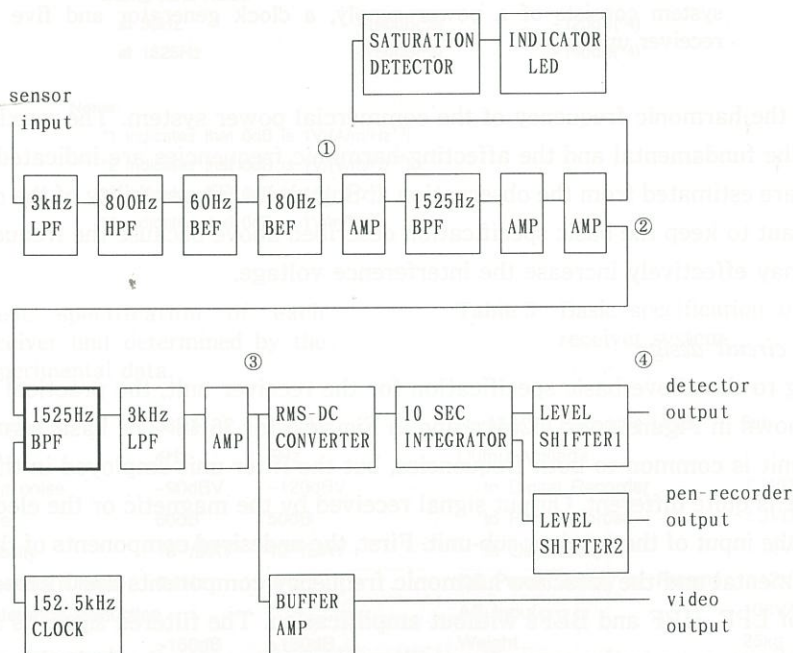


**Fig. 4** A simplified block diagram of one 1525Hz receiver unit. The output of each sensor is connected to the input of this receiver unit. First the wideband signal is filtered by HPF, is rejected at the fundamental and the harmonic frequency components by BEFs, and is amplified approximately 50 dB to fit the signal level of the switched capacitor filters (SCFs). The SCFs tuned to 1525Hz are used to take out the background noise level from the jungle of the power harmonic spectra. The characteristics of the SCFs can be easily set up by trimming the external resistors and the stability of them are kept high with the common crystal oscillator. The output of the narrow band filter is amplified to the suitable amplitude of the RMS-to-DC converter with 10 sec integrator. The converter can convert the AC rms voltage to the DC voltage in the logarithmic sense. The DC amplitude is shifted to the suitable level of the recorders. Additionally the filtered AC signal can be obtained from the output panel. A unique saturation detector can easily indicate the malfunction of the narrow band pass filter.



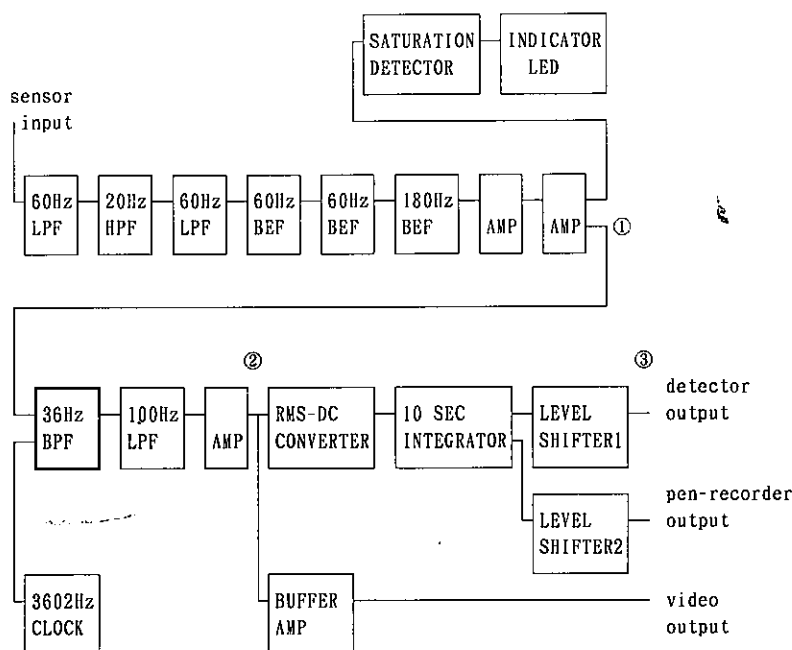


**Fig. 5** A simplified block diagram of 36Hz receiver unit. The structure of the main circuit is almost the same as the 1525Hz receiver unit except for combination filters of the front part of this receiver unit. The 60Hz rejection filters are cascaded to avoid the strong influence of the fundamental frequency induced from the power lines as shown in Fig.1.

was selected as the old type receiver unit(9). The noise reduction ratio is approximately 20dB at 1525Hz.

### 3. Characteristics of the receiver units

#### 3.1 Automatic testing equipment

For testing the performance of the assembled receiver unit, the automatic testing equipment shown in Figure 6 is used. The test system consists of a function synthesizer, an attenuator, a digital multimeter, a spectrum analyzer and an oscilloscope. All of these equipments are connected by the GP-IB cables and are controlled by a personal computer. Frequency and input-to-output characteristics, harmonic distortion and dynamic performance are tested by these equipment, and the test results are filed on the personal computer disk.

#### 3.2 Frequency characteristics

Frequency characteristics of the assembled receiver units are shown as dashed curves in Figure 7 and 8.

In Figure 7, the frequency characteristics at three stages which are corresponding to the same circled figures indicated in Figure 5. Narrow rejection bands at 60Hz and 180Hz can be

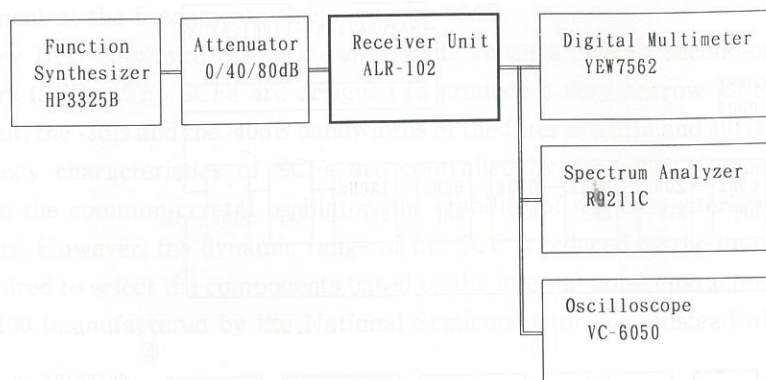


**Fig. 6** A block diagram of testing the performance of the receiver unit. The test system consists of a function synthesizer, an attenuator, a digital multimeter, a spectrum analyzer and an oscilloscope. All of these equipments are connected by the GP-IB cables and are controlled by a personal computer. Frequency characteristics, input-to-output characteristics, harmonic distortion and dynamic performance are tested by these equipment and filed on the personal computer.

clearly seen over the broad BPF characteristics as in Figure 7 ①. The broad-band characteristic is shaped by LPF and HPF combination. Then the broad-filtered signal is again filtered by the medium bandwidth filter centered at 1525Hz with  $Q=20$ . This filter is used to reject the undesired spectrum approximately 200Hz outside of the center frequency. The frequency characteristic is shown in Figure 7 ②. As the analog active filter is not so stable as to shape very narrow BPF with  $Q=400$ , the switched capacitor filter(SCF) which has enough stability is used for the narrow BPF at 1525Hz. The SCF has the stability of  $10^{-5}$ /day since the switching frequency is controlled by the crystal oscillator. The frequency characteristic of the narrow BPF is shown in Figure 7 ③. The  $-3$ dB and  $-40$ dB bandwidth of the narrow BPF is approximately 5Hz and 40Hz, respectively. It can be seen from these characteristics that the detection of the weak background noise at 1525Hz is possible even in the bad location as Sugadaira.

In Figure 8, the frequency characteristics at two stages which are corresponding to the same circled figures in Figure 5. The narrow rejection band at 60Hz can be clearly seen over the wide BPF as in Figure 8 ①. The broad BPF is shaped by the combination of LPF and HPF. The rejection ratio of 60Hz at this stage is approximately 60dB, which is required to suppress the intense induction field at the fundamental frequency as shown in Figure 1. Then the signal is again filtered out by the narrow BPF which is shaped by SCFs. The frequency characteristics of the narrow BPF is shown in Figure 8 ②. The  $-3$ dB and  $-40$ dB bandwidth of the filter is approximately 4Hz and 25Hz, respectively.

### 3.3 Input-to-output characteristics

Input-to-output characteristics of the 1525Hz receiver sub-unit at the three stages, which are corresponding to the same circled figures as in Figure 4, are shown in Figure 9. The lower

saturation level is caused by the internal noise of the receiver sub-unit. The equivalent input noise of this receiver unit is  $-115\text{dBV}$  as seen in Figure 9 ④. As the amplitude at  $1525\text{Hz}$  is

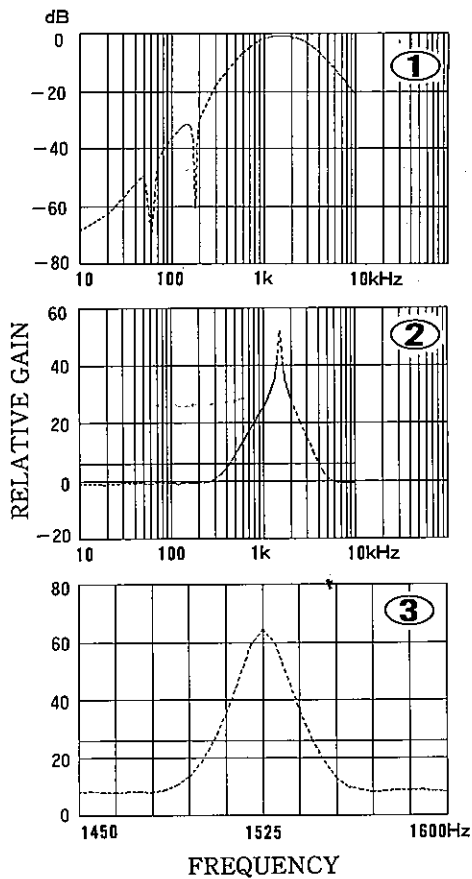


**Fig. 7** Frequency characteristics of a  $1525\text{Hz}$  receiver unit at three stages indicated by the circled figures which correspond to the same circled figures indicated on Fig.4. Narrow rejection bands at  $60$  and  $180\text{Hz}$  can be clearly seen over the wide band pass filter as in ①. The signal is filtered by the medium band pass filter and then amplified as shown in ②. The characteristic of the narrow band pass filter is shown in ③. The  $-3\text{dB}$  and  $-40\text{dB}$  bandwidth of the narrow band pass filter are approximately  $5\text{Hz}$  and  $40\text{Hz}$ , respectively. It can be seen from these characteristics that the detection of the weak background noise at  $1525\text{Hz}$  is possible even in bad location as Fig.1.

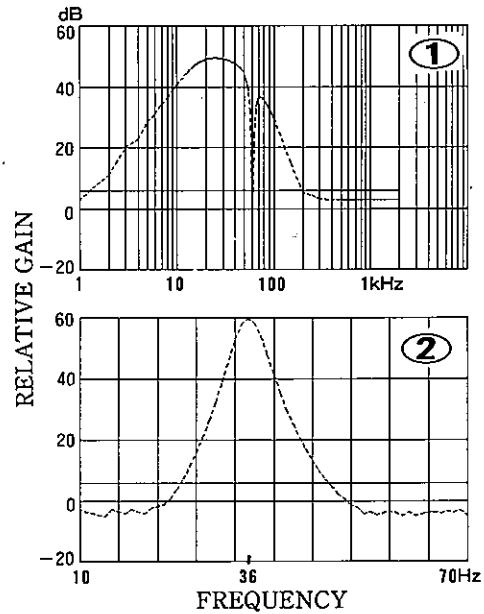


**Fig. 8** Frequency characteristics of one  $36\text{Hz}$  receiver unit at two stages indicated by the circled figures which correspond to the same circled figures indicated in Fig.5. Narrow rejection band at  $60\text{Hz}$  can be clearly seen over the wide pass band as in ①. Amplitude gain from the front top to this stage is approximately  $50\text{dB}$ . The characteristic of the narrow band pass filter is shown in ②. The  $-3\text{dB}$  and  $-40\text{dB}$  bandwidth of the filter are  $4\text{Hz}$  and  $25\text{Hz}$ , respectively.



logarithmically compressed by the RMS-to-DC converter, the output at the stage ④ is converted to  $\pm 1V$ . On the other hand, the upper saturation level is caused by the amplitude saturation of the operational amplifiers for the stage ② and by the amplitude saturation of the SCFs for the stage ③. The equivalent input saturation amplitude is  $-45dBV$ . Consequently the total dynamic range of this receiver sub-unit at  $1525Hz$  is  $70dB$  which is  $20dB$  greater than the designed value.

In Figure 10, input-to-output characteristics of the  $36Hz$  receiver sub-unit is shown. As in Figure 9, the circled figures are corresponding to Figure 5. The lower saturation level is  $-120dBV$  and the upper saturation level is  $-43dBV$ . Then the total dynamic range of this sub-unit is  $77dB$  which is  $17dB$  greater than the designed value.

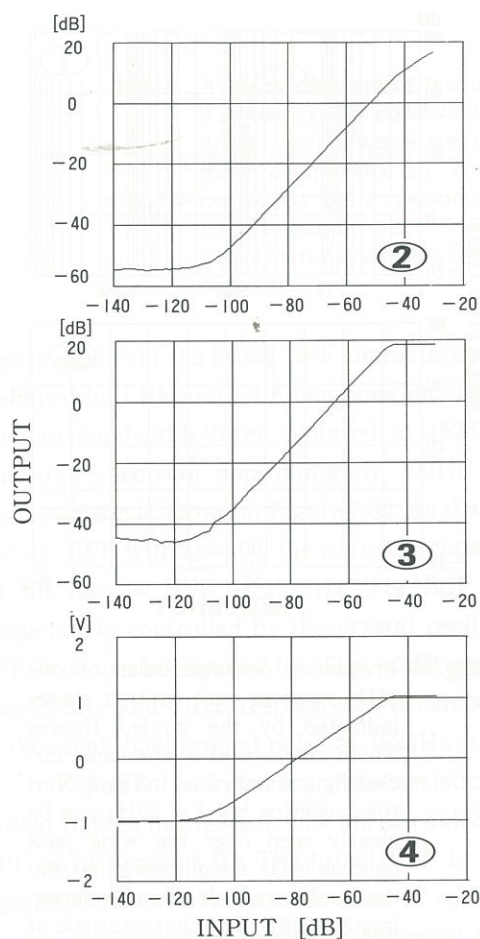


**Fig. 9** Input-to-output characteristics of one  $1525Hz$  receiver unit at three stages. The noise threshold level of this unit is approximately  $-115dB$  for input and the saturation level is  $-45dB$ , therefore, the dynamic range of this unit is  $70dB$ .

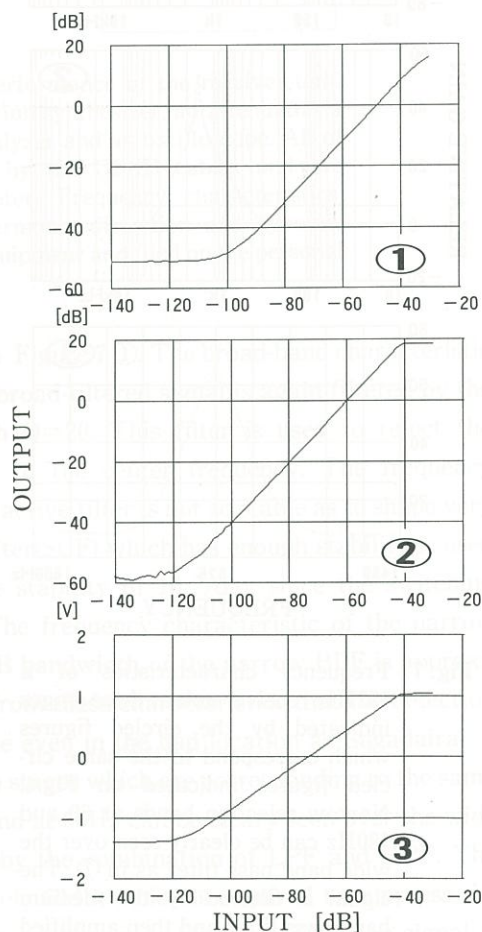


**Fig. 10** The noise threshold level of this unit is approximately  $-120dB$  for input and the saturation level is  $-43dB$ , therefore, the dynamic range of this unit is  $77dB$ .

### 3.4 Comparison of characteristics with the old type receiver units

The characteristics of the newly designed and assembled receiver units are described in the preceding section. Let us compare the characteristics with the old type receiver unit (9) which has been used at Sugadaira since 1989. The frequency characteristics are almost the same as the old type receiver units(9). The rejection rate of the fundamental frequency is increased by 20dB to be used under a severe interference condition. The input-to-output characteristics of the old and the new types of receivers are shown in Figure 11(a) and 11(b), respectively. The dynamic range of the receiver sub-units for the old type receiver is 50dB for the 1525Hz unit or 40dB for the 36Hz unit. The value for the new type one is 70dB for the 1525Hz unit or 77dB for the 36Hz unit. The improvement in the dynamic range is 20dB for 1525Hz unit or 37dB for 36Hz unit. The

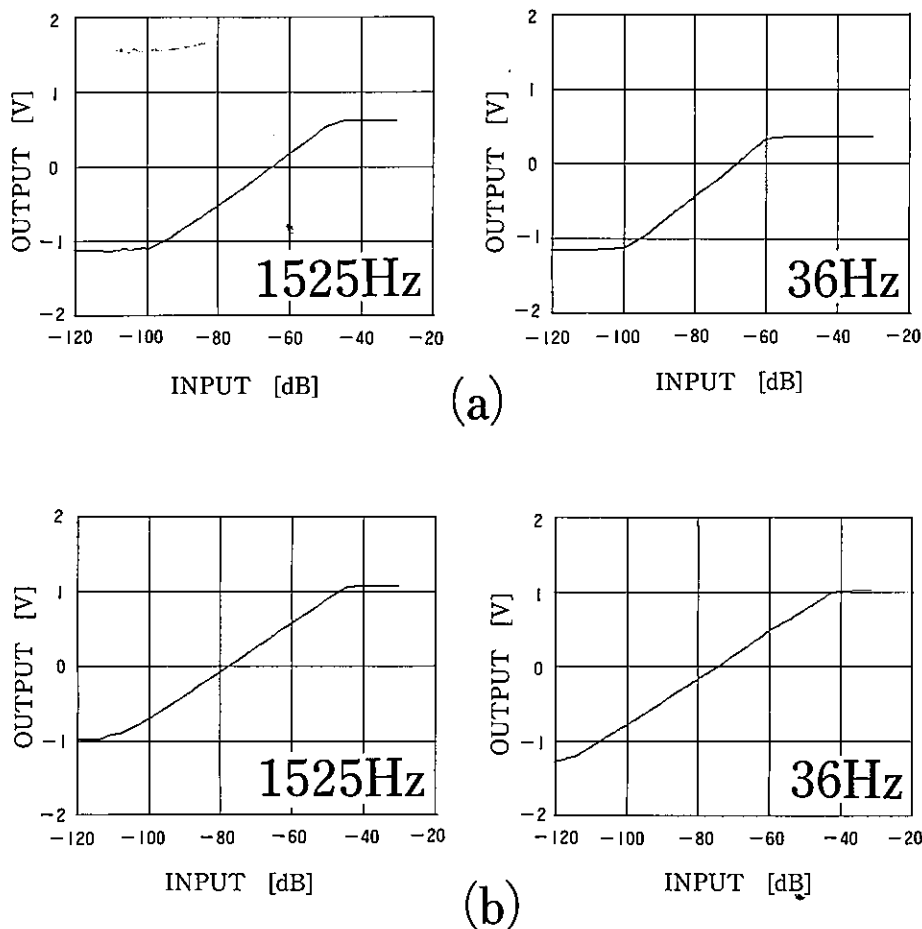


Fig. 11 The input-to-output characteristics of (a) the old type and (b) the new type of receiver unit. The dynamic range of the 1525Hz unit is 50dB and 70dB for the old type and for the new type, respectively. That of the 36Hz unit is 40dB and 77dB for the old type and for the new type, respectively. The improvement in the dynamic range is greater than 20dB for the unit of both frequencies.

great improvement in this characteristic is resulted by selecting SCFs of the least internal noise. Additionally the stability of the receiver unit is obtained by using a common crystal oscillator to control the frequency characteristics of the receiver system without interfering each unit. The new receiver unit is designed and assemble to be compact comparing to the old type one, and the mechanical and electric specification of each unit in this system is assembled to be matched each other to be easily replaced and to be tested under any situation.

#### 4. Evaluation of the receiver performances

##### 4.1 Precision of estimation of the field strength from the output voltage

The ELF receiver system is designed for observing the five field components to detect the relative increase in field strength and the abnormal change in the field strength ratio. The precision of this observation must be affected by the internal errors in the receiver system. The most affective error may be produced by simply converting the output voltage to the field strength due to the non-linearity in the input-to-output characteristics. To reduce the error we have introduced the polynomial fitting method to the conversion process. The number of the polynomials is 10 for this process. Examples of the polynomial fitting are shown in Figure 12 for both frequencies. The resulted estimation error in this case is 0.031dB for 1525Hz unit or 0.019dB for 36Hz unit. It is sufficient to observe the abnormal phenomena associated with earthquakes or volcanic eruptions since the normal and natural amplitude fluctuation is approximately 1dB

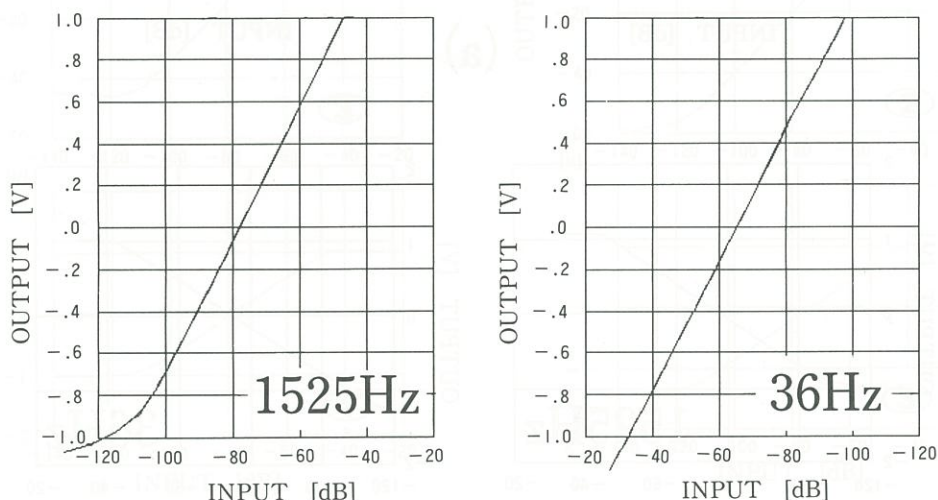


**Fig. 12** Curves for the 1525Hz and the 36Hz receiver units fitted by the polynomial functions which are calculated from the input-to-output characteristics shown in Fig.11(b). The expected fitting error of this function is 0.031dB for the 1525Hz and 0.019dB for the 36Hz units. These conversion functions are used for calculating the equivalent electric or magnetic field strengths by taking the sensitivity of the sensor units and the bandwidth into account.



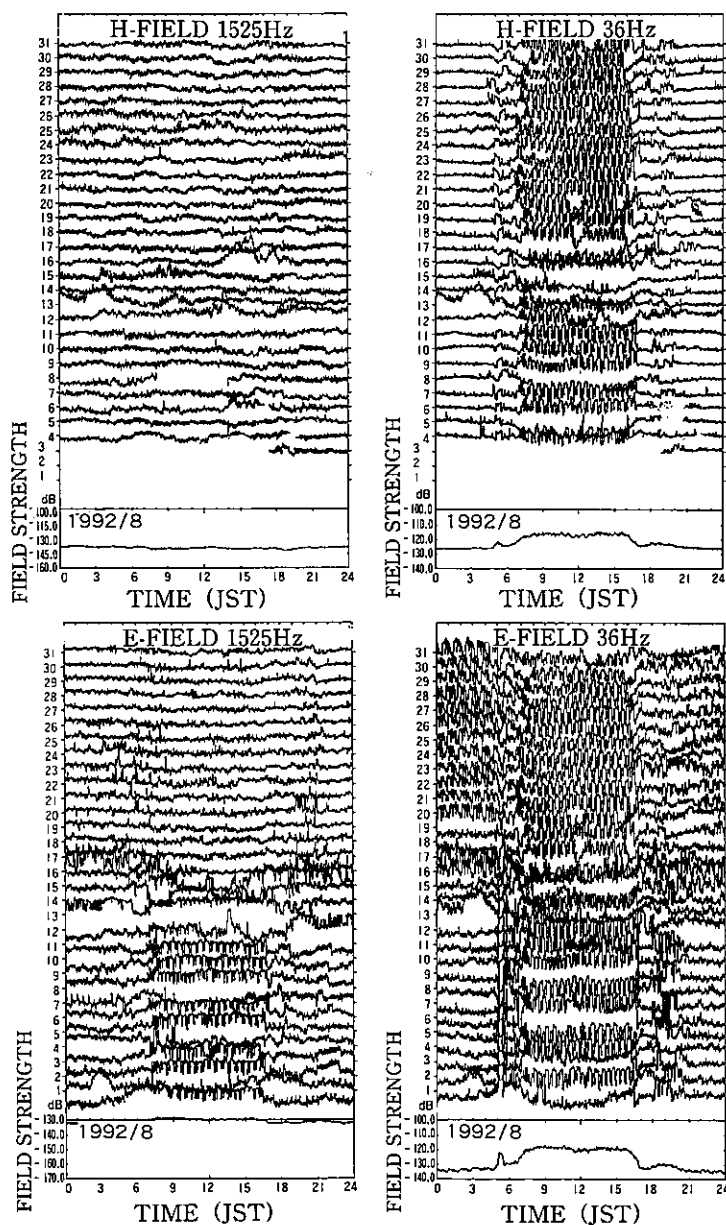


Fig. 13 An example of the compiled data obtained at Kunimi-cho near the Unzen Volcano, which is actively erupting since 1991. Format of the data is same for four panels. The monthly average of the daily variation of field strength at each component is shown at the bottom of each panel. The field strength is indicated by dB relative to  $1\text{A/m/Hz}^{1/2}$  and  $1\text{V/m/Hz}^{1/2}$  for the magnetic and the electric field, respectively. The daily variations with respect to the monthly average value are indicated on the upper part of each panel. The day number of the month is indicated on the left side of each curve. Very high interference in the daytime can be clearly seen except for the 1525Hz magnetic field, however, it is relatively quiet during the nighttime.

for the interval of 10 seconds at the ELF range(9).

#### 4.2 *An example of observation made at Kunimi-cho near the Unzen Volcano*

The ELF receiver system is first designed to be used at the Kunimi observation point north-west of the Unzen Volcano, where we have been observing the EM phenomena associated with earthquakes or volcanic eruptions since 1991. The activity of the volcano is so high since May, 1991 that we can expect EM phenomena associated with these events. The distance from the most active volcano to the observation point is 4km. The observation point is just on the Chijiwa fault which indicates the high activity. The ELF receiver system was set up in June 1992 with the recording system. Although there has been no special event to be related to our observation since then, the ELF receiving system is continuously working without serious trouble. Therefore the stability of the system can be confirmed by this result. An example of observation at Kunimi station is shown in Figure 13 as for the normal condition. Although we have been observing the five field components, only two components, north-south electric and magnetic, both for 1525Hz and for 36Hz are shown. The format of display is same for these four panels. At the bottom of each panel the monthly averaged value of one-day field variation is shown with the absolute field strength on the left side. The daily variation relative to this monthly averaged value is shown at the upper part of each panel. The field strength is indicated by dB relative to  $1\text{A/m/Hz}^{1/2}$  and  $1\text{V/m/Hz}^{1/2}$  for the magnetic and for the electric field, respectively. The day number of the month is indicated on the left side of each curve. Very high level field in the daytime can be clearly seen except for the 1525Hz magnetic field. The high level field must be correlated to the artificial noise since it shows the clear daytime enhance and the constant start and end time. As we have designed not to be disturbed by the high interference field at the harmonic frequencies of the commercial power system, this high level field may be caused by other type of interference such as electric motor or electric inverter. However, a small abnormal change can be detected during the nighttime when the high level of interference does not appear.

### 5. Summary

According to our experience in the observation of EM phenomena associated with earthquakes or volcanic eruptions, a new type of the ELF receiver system is designed. The receiving frequencies in the ELF band are fixed by the characteristics of the test observation at Sugadaira Space Radiowave Observatory in Nagano Prefecture. Other design parameters such as the rejection ratio and the background noise strength is also determined at the same test observations since the fundamental frequency is 60Hz, which is the same condition as Kunimi-cho near the Unzen Volcano. The design of the new ELF receiver system is mainly focused on the high rejection ability for the interference induced by the commercial power system, on the high dynamic range, on the stability, and on the operability.

The actual characteristics of assembled receiver units are measured by the automatic test equipment controlled by GP-IB to perform a complex procedure during the measurement. The

frequency characteristics show sufficient rejection rates to the assumed interference frequencies. The dynamic range of the units can be measured from the input-to-output characteristics as the difference between the internal noise voltage to the saturated voltage. The resulted values for the dynamic ranges are 70dB for 1525Hz unit and 77dB for 36Hz unit, which is approximately 20dB greater than the designed value. The expansion of the dynamic range is attained by the selection of SCF ICs for the lower internal noise. The comparison between the old type of receiver and the newly assembled one indicates the improvement in the rejection rate, the dynamic range, the stability and the operability.

As the newly developed ELF receiver system has been successfully operated for more than three month at the field station placed near the Unzen Volcano, the performance of the system can be confirmed. Data processing of the observation data recorded at the Kunimi station is now in progress by applying the direction finding method developed by Hayakawa et al. (10).

Acknowledgements: The development of the ELF receiver system was supported by the Grand-in-Aid of the Ministry of Education, Science and Culture, Japan, number 03201123. The authors thank to Any Co. Ltd. for the aid in assembling the receiver system.

### References

- 1) Gokhberg, M. B., Morgounov, V. A., Yoshino, T., and Tomizawa, I. : J. Geophys. Res., **87**, 7824-7828 (1982)
- 2) Yoshino, T., Tomizawa, I., and Shibata, T. : Ann. Geophys., **3**, 727-730 (1985)
- 3) Yoshino, T., and Tomizawa, I. : IEICE Tech. Rep., EMCJ88-64 (1988)
- 4) Yoshino, T., and Tomizawa, I. : J. Geomag. Geoelectr., **22**, 225-235 (1990)
- 5) Yoshino, T., Tomizawa I., Hayakawa, M., and Seo, Y: Proc. Spring Meeting of SGEPS (1992)
- 6) Tomizawa, I. : Proc. Soc. Atmos. Electr. Japan, **no. 40**, 23-28 (1992)
- 7) Yamada, I. : Ph. D thesis, Nagoya University (1990)
- 8) Schumann, W. O. : Z. Naturforsch., **7A**, 149-154 (1952)
- 9) Sugimoto, T.: Master Thesis, the University of Electro-Communications (1991)
- 10) Haykawa, M., Tomizawa, I., Ohta, K., Shimakura, S., Fujinawa, Y., Takahashi, K., and Yoshino, T. : Phys. Earth Planet. Interior, in press (1992)